J Nanostruct 16(2): 1744-1751, Spring 2026

RESEARCH PAPER

Tunable Morphologies and Optical Properties of ZnS Nanostructures Doped with Ni, Co, and Mn: A Solvothermal Synthesis Approach

Fadhel H. Ali [1] *, ***Asraa T. Nasser*** [2], ***Hussein M. Hussein*** [3,4]

[1] *Physics Department, College of science, University of Babylon, Babylon, Iraq*

[2] *Department of Chemical Engineering, Faculty of Engineering, Kufa University, Kufa, Iraq*

[3] *Department of Physics, Faculty of Education for Women, Kufa University, Kufa, Iraq*

[4] *Medical Physics Department, Hilla University College, Babylon, Iraq*

ARTICLE INFO

Article History:
Received 12 December 2025
Accepted 21 March 2026
Published 01 April 2026

Keywords:
Doped and undoped ZnS
Magnetic study
Morphological effects
XRD study

ABSTRACT

Due to λ > 340 nm of ATC metallation ligands SSF also marks an important event because it was the first synthesized mono-metallic crystalloid with such readiness used generally as organolithium sparepart even now; after Co-rich treatment, obviously. After that the nanostructures were functionally characterized (mainly structure, optical, morphological and magnetic) systematically such as XRD, and FESEM. The results indicated that morphology manipulation plays a critical role in improving the functional properties of ZnS. The dopant-induced enhancement type and extent were largely variable depending on the electronegativity and ionic radii of the dopants, leading to significant variation in lattice parameters, band gap energies as well as light absorption behaviours. Magnetic characterization proved that among the various dopant ions, which facilitated an homogeneous distribution in purified ZnS lattice, improved magnetic behavior and resulted in smaller crystal as well as average grain size of ZnS. The coercively and the remnant magnetization were also increased with this structural refinement than that of pure ZnS. Within the doped forms, individual transition metals contributed unique benefits, resulting in tailored optical and magnetic responses. Finally, the investigations done here emphasized that Ni-, Co- and Mn-doped ZnS nanostructures displayed better multifunctional performance as compared to undoped ZnS, which revealed them as potential material for implementation in optoelectronic device applications. Apparently, the structural stability, improved magnetic properties and adjustable optical transparency of the Co-Nis make them interesting as potential buffer layer replacements in thin-film solar cells with possible enhancements on device performance coupled with material lifetime.

How to cite this article
Ali F., Nasser A., Hussein H. Tunable Morphologies and Optical Properties of ZnS Nanostructures Doped with Ni, Co, and Mn: A Solvothermal Synthesis Approach. J Nanostruct, 2026; 16(2):1744-1751. DOI: 10.22052/JNS.2026.02.026

* *Corresponding Author Email: sci.fadhel.hasan@uobabylon.edu.iq*

INTRODUCTION

Diluted magnetic semiconductors (DMSs) can be produced by substituting transition metal ions with doping of semiconductor nanostructures [1-4]. DMSs are estimate one of the most hopeful candidate materials for spintronic applications because of their nanostructure and crystalline nature, which manifest novel electro-optical and magnetic properties [5-7]. ZnS-based DMS is widely studied [8-11] due to the high solubility of magnetic atoms in the II– VI host lattice, and these materials can be ferromagnetic when transition magnetic ions are induced into the host ZnS [12]. The optical energy band gap of the ZnS compound is about 3.6 eV [13-15]; Therefore, it represents un optimum candidate for utilizing in electroluminescence, cathode luminescence [16], and sensors devices. Doping with this compound leads to other characteristics and this depends largely on the type of impurity ions. The impurity ions occupy the Zn lattice and act as electron–hole traps within the optical bandgap between the VB. and CB. In fact, nickel, manganese, and cobalt dopant elements possess magnetic properties that enhance crystalline growth when these dopants are introduced into the crystal structure of a material, as reported previously [17-20]. This enhancement is critical to the tuneable morphology of the nanoparticles, which significantly affects the physical properties of the crystal structure. Therefore, herein, the authors report how the dopant elements Ni, Mn, and Co are synthesised with doped ZnS nanostructures, and then investigate how the structural, morphological, optical, and magnetic properties are affected by incorporating these dopants into the host ZnS. The main idea of improving the characteristics of the zinc sulfide compound is to change the morphology of nanoparticles from sphere-like to rod-like, flower-like, and sheet-like nanoparticles, which in turn provide new properties of the ZnS nanostructure.

MATERIALS AND METHODS

The Ni, Mn, and Co dopant elements were doped with pure ZnS nanospheres and synthesized using the solvothermal method. All precursors were purchased from Merck. In general, 0.13632, 0.12959, 0.25844, and 0.12984g from $ZnCl_2$, $NiCl_2$, $MnCl_2$, and $CoCl_2$ precursors were synthesized to prepare doped and undoped ZnS nanoparticles. Using 0.32g of capping agent (polyvinylpyrrolidone), It was resolved in 40 ml of EG as solvent with regular stirring for 3 h at 80 °C. The produced resolution was carried into an autoclave and then het up at 250°C in an oven

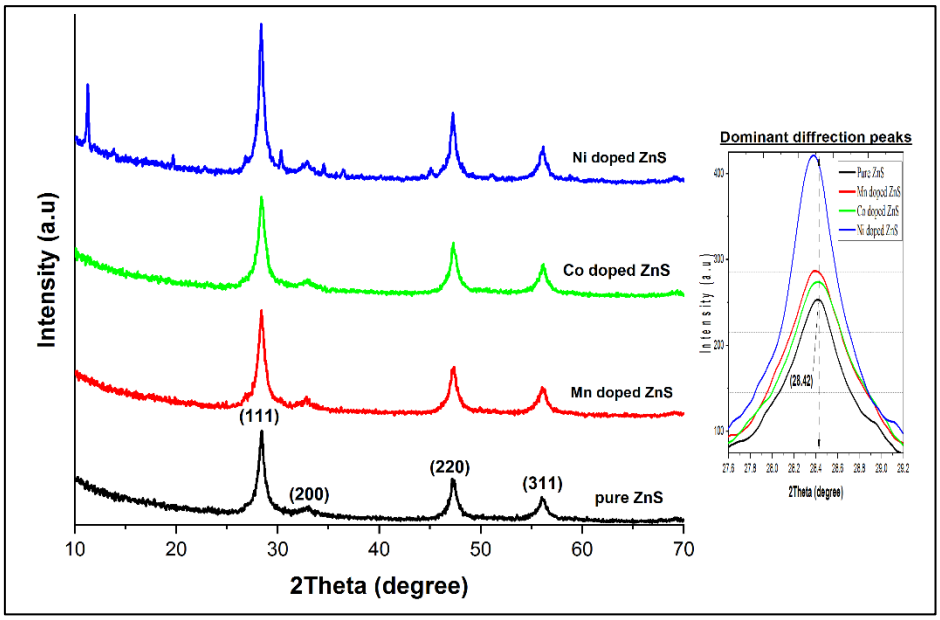

Fig. 1. XRD pattern of pure ZnS and Ni/Mn and Co doped ZnS

for 6 hours. The autoclave is then cooled to room temperature. Finally, by washing the sediments with distilled water, mixing them with absolute ethanol many times, and then drying them at 80 °C for 2 h in a vacuum oven, the resulting product is a nano-powder.

Characterization

Doped and undoped zinc sulphide nanostructures were characterised by XRD patterning with Cu-Kα radiation (λ=0.15406 nm) (D8 Advance Bruke). FESEM (Zeiss, PIJMA-VP) was performed to observe the morphology of the nanoparticles. UV-Vis spectroscopy (shimadzu UV-1800) was used to study the optical properties. Finally, a vibrating sample magnetometer (Lakeshore VSM-7410) was used to investigate the behaviour of the magnetic and the doped ZnS nanoparticles properties.

RESULTS AND DISCUSSION

XRD pattern study

Fig. 1 shows the XRD patterns of the synthesized pure ZnS and x-doped ZnS (x=Ni, Mn and Co) nanoparticles. Each sample exhibits a single phase (cubic zinc blend) structure without detectable secondary phase formation, confirming the successful incorporation of dopants into the ZnS lattice. It was observed that the dominant diffraction peaks, located at the 2θ positions 28.42°, 47.50°, and 56.35° indexed to the diffractions of (111), (200), (220), and (311) planes, and which matches the standard JCPDS card number 89-7385, as summarised in Table 1. It can be seen that doping with nickel, manganese and cobalt does not later the lattice structure of the pure ZnS, but affect the crystal structure parameters, and induces subtle modification in the lattice parameters. This effect can be observed in the tiny diffraction peaks in the nickel-doped ZnS. Moreover, the slight shifts of the dominant diffraction peaks of the pure ZnS toward lower angles (inset of Fig. 1), indicative of lattice expansion according to Bragg's law.

This means that the dopant cations occupy the Zn cation position in the crystal lattice. The smaller ionic radius of Ni^{2+} (0.69Å) than that of the Zn^{2+} (0.74Å) would be expected to contract the lattice, shifting peaks to higher angles. However, the observed shift toward lower angles reveal that defect formation such as Zn or S vacancies along with local strain effects, counterbalances the anticipated contraction. This may be due to the magnetic property of nickel, which affects the redistribution of cations and then the lattice strain of the unit cell. The larger ionic radius of Mn^{2+} (0.80Å) inherently expands the lattice, while the ionic radius of Co^{2+} (0.745Å) nearly identical to Zn^{2+}, induces minimal volumetric change, with strain related distortion demonstrating its structural impact [21]. The size of crystal D was evaluated from the dominant XRD peak using the Debye–Scherrer formula [22] $D=0.94\lambda/\beta\cos\theta$, where β is the full width at half maximum of the dominant XRD peak, and θ is the position of the diffraction peak. The Table 1 summarizes, the values of lattice parameter "a", unit cell volume "V", and crystallite size "D". in the Ni^{2+} doped ZnS sample slight reduction in "a", "V" and "D", with increased strain. In the Mn^{2+} doped ZnS sample exhibits the highest strain and the smallest crystallite size, consistent with lattice expansion coupled with substantial micro-strain from ionic radius mismatch. While, Co^{2+} doped ZnS sample reveals minimal change in "a" and "V" but significant strain and reduced crystallite size indicating defect induced distortion as the dominant effect [22]. In all doped samples, the crystallite size decreases relative to pure ZnS, suggesting that dopant incorporation hinders

Table 1. The crystalline parameters of pure ZnS and Ni/Mn and Co doped ZnS

Sample	Dominant diffraction peak "2θ" degree	Lattice constant "a" Å	The unit cell volume "V" nm	Crystallite size "D" nm	Strain
Pure ZnS	28.42	5.4372	160.74	9.586	0.0147
Ni doped ZnS	28.37	5.4363	160.66	9.217	0.0153
Mn doped ZnS	28.39	5.4344	160.49	7.836	0.0180
Co doped ZnS	28.41	5.4369	160.71	7.895	0.0179

crystal growth during nucleation. The concurrent increase in microstrain values reflects enhanced lattice distortion, which is expected to influence carrier transport, defect state density, and consequently, the optical performance of the materials.

Morphological study

The shape of nanoparticles of the undoped and doped ZnS nanoparticles was observed by FESEM, as shown in Fig. 2. For Pure ZnS, the nanoparticles show spherical morphology in a consistent and uniform shape and size with large agglomeration may be ascribed to the high surface energy and van der Waals forces.

Upon doping process was incorporated into host ZnS, the nanoparticle morphology changed from spherical to rod-like, flower-like (hierarchical assemblies), and thin nanosheet-like morphologies in Ni, Co, and Mn-doped ZnS, respectively (Fig. 2a-d).

From the XRD patterns and according to the relationship of nanoparticle size, it was observed that the particle size decreases with the incorporation of dopants, as summarized in Table 2. Decreasing the particle size was accompanied by an increase in dislocation density with the incorporation of dopants into the host's ZnS, resulting in a raise in the lattice strain of the structure. This substitution leads to local distortions in the lattice, which act as nucleation centers, changing the crystal growth kinetics and

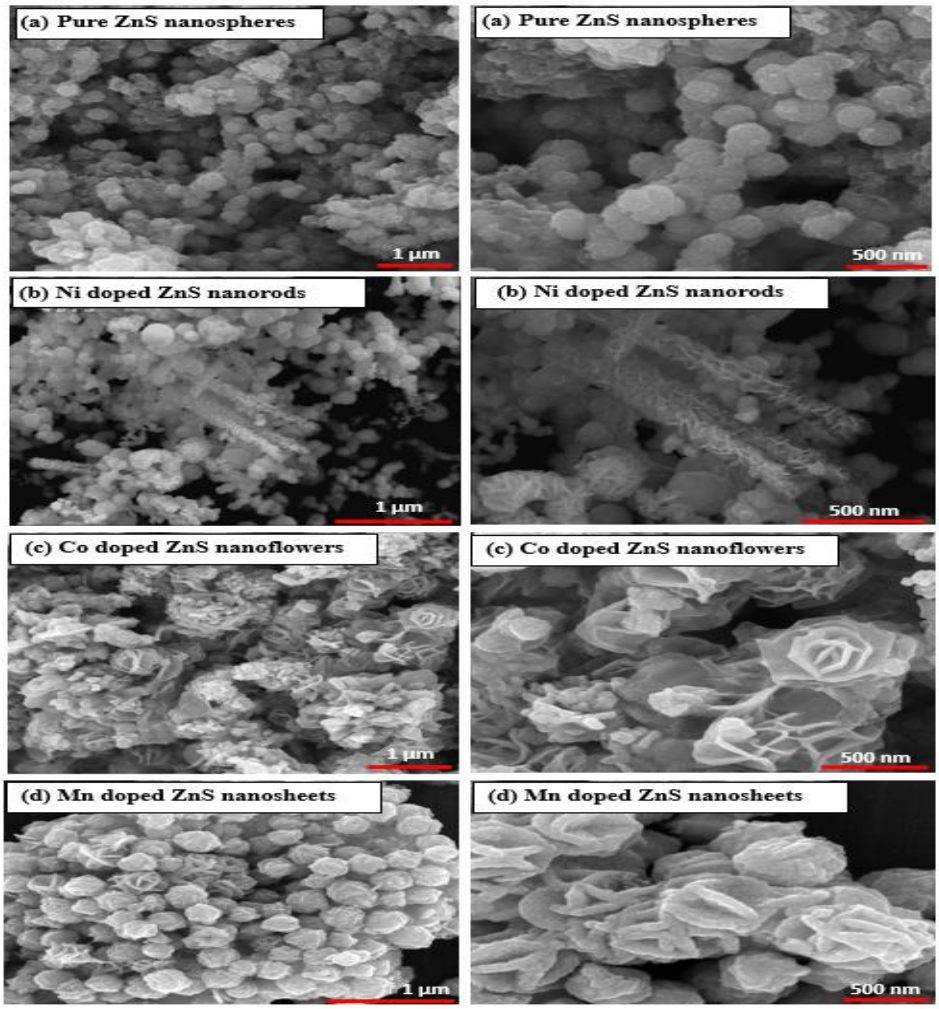

Fig. 2. Morphology of nanoparticles for pure ZnS (a), Ni doped ZnS (b), Co doped ZnS (c) and Mn doped ZnS (d)

thus the final shape of the nanoparticles.

This transformation in the nanoparticles shape was accompanied by an increase in defects with a decrease in crystal size. The altration in particle shape from spherical to rod, flower, and sheet is as a result of the decrease in pressure inside the unit cell, this in turn results in less cation disorder in the crystal structure because of the ionic radius of the doped ions compared to the ionic radius of Zn^{+2}. Based on what was mentioned, the effect of doping on the ZnS by changing the shape of the nanoparticles may help enhance the optical properties of the ZnS particles. Morphological variation suggests that similitudes influence the anisotropic growth rates of zinc sulfide (ZnS) crystal planes, due to changes in surface energy and preferential adsorption of similitude ions on specific crystal faces. Controlling the shape of nanoparticles can have a profound impact on the physical and functional properties of ZnS nanostructures. For example, anisotropic structures, such as nanorods and nanosheets,

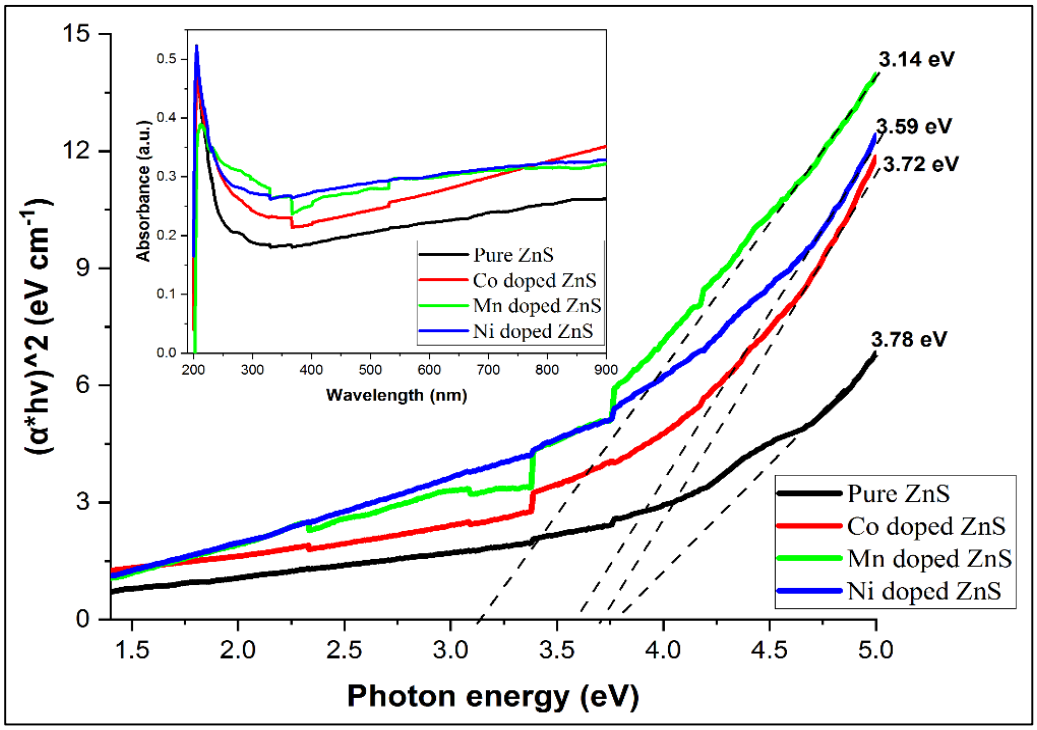

Fig. 3. Absorption spectrum and energy band gap of pure ZnS and Ni/Mn and Co doped ZnS

Table 2. Morphological characteristics of pure ZnS and Ni/Mn and Co doped ZnS.

Sample	Particles size (nm)	Dislocation density=1/D^2 (nm^{-1})	Strain
Pure ZnS	63.00	0.0109	0.0147
Ni doped ZnS	60.91	0.0116	0.0153
Mn doped ZnS	51.50	0.0163	0.0180
Co doped ZnS	51.89	0.0160	0.0178

typically exhibit enhanced charge carrier transport and increased surface-to-volume ratio, which improves photocatalytic and optoelectronic performance.

Optical study

UV– visible spectroscopy was utilized to investigate the optical properties of the pure ZnS and doped ZnS nanoparticles. It was noticed that the doping process leads to the insertion of intermediate states between the conduction and valence bands, which may enhance the optical properties of the material. As shown in Fig. 3, the absorbance of the pure ZnS is improved when the dopant elements are introduced into the host's ZnS due to the induction of additional optical levels within the forbidden gap, which in turn leads to rise the optical transitions and improved absorbance. The morphology of the nanoparticles is another reason for improving the optical property of the zinc sulfide compound. It was found that rod-like, flower-like, and sheet-like nanoparticles are preferred over spherical-like nanoparticles because of their hierarchical assembly, crystallinity, and tunable geometrical parameters, which in turn leads to an increase in the absorption coefficient of the material.

Furthermore, the optical band gap contributes to the enhancement of the absorbance intensity and the broad band of the wavelengths. As shown in Fig. 3, when dopant elements are incorporated into the structure of the zinc sulphide, the optical band gap decreases from 3.78 eV to 3.72 3.59 eV and 3.14 eV for pure ZnS, Co-doped ZnS, Ni-doped ZnS, and Mn-doped ZnS, respectively. The energy band gap (Eg) was deduced according to the Tauk's relation [22] αhv=A(hu-Eg) where A is a constant, α is the absorption coefficient and h is plank's constant. By plotting of $(\alpha hv)^2$ vs the photon energy (hu) and taking the intercept on the hv-axis, the optical band gap can be estimated. Electronegativity affects the optical property of the material through hybridisation between cations and anions. The electronegativity of an atom is strongly correlated with the ionisation energy. Therefore, electrons with high ionisation energies have low electronegativity, as in the Zn element, because their nuclei do not exert a strong attractive force on electrons. Elements with low ionisation energy, such as the dopant elements Ni, Mn, and Co, have higher electronegativity, which resulted in stronger ionic interaction of Dopant-S

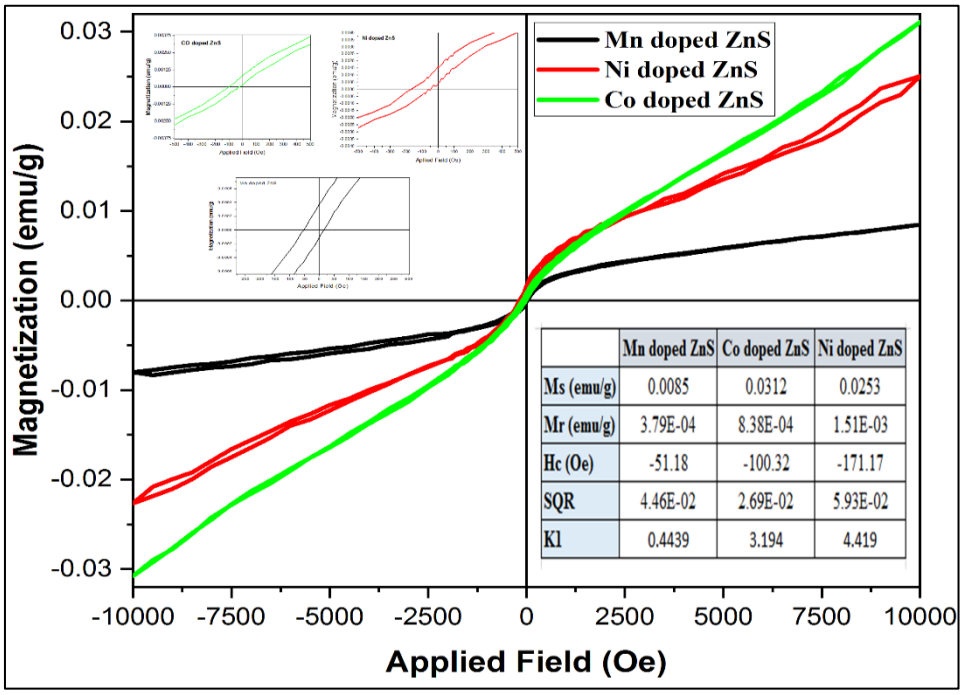

	Mn doped ZnS	Co doped ZnS	Ni doped ZnS
Ms (emu/g)	0.0085	0.0312	0.0253
Mr (emu/g)	3.79E-04	8.38E-04	1.51E-03
Hc (Oe)	-51.18	-100.32	-171.17
SQR	4.46E-02	2.69E-02	5.93E-02
Kl	0.4439	3.194	4.419

Fig. 4. Magnetization *vs* applied field curve of Ni/Mn and Co doped ZnS nanoparticles at room temperature.

compared with Zn-S.

Magnetic study

The magnetic property of the Ni/Mn- and Co-doped zinc sulfide nanostructures were investigated by VSM, as shown in Fig. 4. It shows the magnetization *vs* the applied magnetic field measured at room temperature. The weak magnetic hysteresis loops indicate that all samples are ferromagnetic at room temperature. It was found that changing the morphology of nanoparticles results from incorporating magnetic elements into the ZnS host, which results in an increase in the magnetic property of the material through increasing saturation magnetization Ms. The crystal size or particle size of the Ni-doped ZnS sample represents the critical size at which coericivity H_c is high. Therefore, it can be said that the coericivity and remnant magnetization M_r increases with decreasing crystal size or particle size before reaching the critical size due to the strong spin interaction during nanoparticle alignment and hence transforms from a single domain region to a multi-domain region.

There is a relationship between the coericivity Hc of the material and grain size. where increasing the value of Hc means that more energy is required for demagnetisation of the material, i.e., increasing the grain boundaries accompanied by decreasing the grain size. To investigate the state of nanoparticles in a single magnetic domain or multi-magnetic domain, the sureness ratio of the material was determined according to the relation SQR=Mr/Ms [23]. I It was found that all samples have an SQR> 0.5 at which the samples are in the multimagnetic domain. In addition, the Co-doped ZnS sample exhibited higher disordering than the other samples because of its smaller SQR value. In addition, the coericivity of the material has an important effect on the anisotropy of the properties in any crystal, as shown in relation K1=(Mr×Hc)/0.98 [23], where K1 is the magnitude of the anisotropy constant. It was found that the Mn-doped ZnS sample had a smaller anisotropy than the Co/Ni-doped ZnS samples.

CONCLUSION

Pure ZnS, Ni/Mn, and Co-doped ZnS nanoparticles were successfully synthesized using the solvothermal method. The incorporation of the dopant elements Ni, Mn, and Co into the ZnS nanostructure plays an important factor in the crystal growth and morphology of nanoparticles. The nanoparticles of each sample exhibit a cubic zinc blende structure without any secondary phase formation. Crystalline parameters such as the lattice constant, unit cell volume, and crystalline size decreased with the incorporation of dopant elements into the host's ZnS, accompanied by increased the lattice strain within the volume of unit cell. Morphology of the nanoparticles changed from spherical-like in the pure ZnS nanoparticles to rod-like, flower-like, and sheet-like in the Ni, Co, Mn doped ZnS nanoparticles, respectively, resulting in an increase in the optical transitions and an improvement in the absorption coefficient. In addition, the magnetic study showed that the as-synthesized Ni, Mn, and Co-doped ZnS nanoparticles exhibited ferromagnetism at room temperature. This result denoted that dopant elements significantly influence the ZnS compound and may improve its optical properties.

ACKNOWLEDGMENTS

The authors thank university of kufa, and Hilla university college, and the authors state that there is no competing interest.

CONFLICT OF INTEREST

The authors declare that there is no conflict of interests regarding the publication of this manuscript.

REFERENCES

1. Prasad AS. Green synthesis of nanocrystalline manganese (II, III) oxide. Mater Sci Semicond Process. 2017;71:342-347.
2. Choi HJ, Seong HK, Chang J, Lee KI, Park YJ, Kim JJ, et al. Single-Crystalline Diluted Magnetic Semiconductor GaN:Mn Nanowires. Adv Mater. 2005;17(11):1351-1356.
3. Zhao Q, Xiong Z, Luo L, Sun Z, Qin Z, Chen L, et al. Design of a new two-dimensional diluted magnetic semiconductor: Mn-doped GaN monolayer. Appl Surf Sci. 2017;396:480-483.
4. Yatsunenko S, Świątek K, Godlewski M, Fröba M, Klar PJ, Heimbrodt W. Electron spin resonance investigations of ZnMnS nanoparticles. Opt Mater. 2008;30(5):753-755.
5. Çolak Ş. Electron Spin Resonance Spectroscopy Investigations on Radiosterilization Feasibilities of Sulfadiazine, Sulfamethoxydiazine and Sulfaquinoxaline. Electron Spin Resonance Spectroscopy in Medicine: Springer Singapore; 2018. p. 83-101.
6. Dhonde M, Sahu K, Murty VVS. Cu-doped TiO_2 nanoparticles/graphene composites for efficient dye-sensitized solar cells. Solar Energy. 2021;220:418-424.
7. Hu H, Zhang W. Synthesis and properties of transition metals and rare-earth metals doped ZnS nanoparticles. Opt Mater. 2006;28(5):536-550.
8. Furdyna JK. Diluted magnetic semiconductors. J Appl Phys.

1988;64(4):R29-R64.
9. Sarkar I, Sanyal MK, Kar S, Biswas S, Banerjee S, Chaudhuri S, et al. Ferromagnetism in zinc sulfide nanocrystals: Dependence on manganese concentration. Physical Review B. 2007;75(22).
10. Owens FJ, Gladczuk L, Szymczak R, Dluzewski P, Wisniewski A, Szymczak H, et al. High temperature magnetic order in zinc sulfide doped with copper. Journal of Physics and Chemistry of Solids. 2011;72(6):648-652.
11. Eryong N, Donglai L, Yunsen Z, Xue B, Liang Y, Yong J, et al. Photoluminescence and magnetic properties of Fe-doped ZnS nano-particles synthesized by chemical co-precipitation. Appl Surf Sci. 2011;257(21):8762-8766.
12. Stern RA, Schuler TM, MacLaren JM, Ederer DL, Perez-Dieste V, Himpsel FJ. Calculated half-metallic behavior in dilute magnetically doped ZnS. J Appl Phys. 2004;95(11):7468-7470.
13. Madhavi J, Prasad V. ZnS and ZnS/CdS core-shell Nano particles: Synthesis, properties and Perspectives. Surfaces and Interfaces. 2020;21:100757.
14. Çiriş A, Başol BM, Atasoy Y, Küçükömeroğlu T, Karaca A, Tomakin M, et al. Effect of CdS and CdSe pre-treatment on interdiffusion with CdTe in CdS/CdTe and CdSe/CdTe heterostructures. Mater Sci Semicond Process. 2021;128:105750.
15. Ahmed KK, Hussen SA, Aziz SB. Transferring the wide band gap chitosan: POZ-based polymer blends to small optical energy band gap polymer composites through the inclusion of green synthesized Zn^{2+}-PPL metal complex. Arabian Journal of Chemistry. 2022;15(7):103913.
16. Bai H, Zhang J, Wang H, Xiang Y, Lu S. Highly conductive quaternary ammonium-containing cross-linked poly(vinyl pyrrolidone) for high-temperature PEM fuel cells with high-performance. J Membr Sci. 2022;645:120194.
17. Hussein HM. Comparative Study between Spin Coated Cu_2ZnSnS_4 and Cu_2FeSnS_4 Thin Films for Thin-Film Solar Cell Applications. Applied Solar Energy. 2022;58(6):751-759.
18. Hussein MH. Fabricating and Synthesizing Spin Coated CuO Thin Film as Absorber Layer in Optoelectronic Applications. Protection of Metals and Physical Chemistry of Surfaces. 2023;59(3):422-427.
19. Hussein MH. Structural and Optomagnetic Properties of Ni-Doped ZnS Synthesized by Solvothermal Method. Colloid J. 2023;85(4):666-672.
20. Venkatarao K, Tirumala Rao B, Sreedevi G, Nirmal Rajeev Y, Cole S. Spectral and structural properties of CuO doped ZnS-MoS_2 nanocomposites synthesized by hydrothermal method. Materials Today: Proceedings. 2023.
21. Hussein H, Yazdani A. Doping the bismuth into the host's Cu_2ZnSnS_4 semiconductor as a novel material for thin film solar cell. Results in Physics. 2019;12:1586-1595.
22. Hussein H, Yazdani A. Spin-coated Cu_2CrSnS_4 thin film: A potential candidate for thin film solar cells. Mater Sci Semicond Process. 2019;91:58-65.
23. Jahan N, Uddin MM, Khan MNI, Chowdhury FUZ, Hasan MR, Das HN, et al. Impact of particle size on the magnetic properties of highly crystalline Yb^{3+} substituted Ni–Zn nanoferrites. Journal of Materials Science: Materials in Electronics. 2021;32(12):16528-16543.